4A.4

THE MEAN STRUCTURE OF VERTICAL VELOCITIES AND RADAR REFLECTIVITIES IN THE HURRICANE EYEWALL AS THEY RELATE TO ENVIRONMENTAL WIND SHEAR

Michael L. Black, Frank D. Marks, Jr., and Robert F. Rogers, NOAA/AOML/HRD
Lynn K. Shay and Bruce A. Albrecht, RSMAS/MPO, University of Miami
Hugh E. Willoughby, International Hurricane Center, Florida International University

1. INTRODUCTION

Vertical shear of the environmental wind has long been known to be a primary modulator of tropical cyclone (TC) structure and intensity. It has only been in the last decade, however, that quantitative analyses of the effects of shear have been prominent in the literature. Much of this work has been realized with analytical and numerical models of the TC in an idealized environment (e.g., Jones 1995, Frank and Ritchie 2000). There has also been additional insight into our understanding of the effects of shear on TC structure from individual case studies of hurricanes (Reasor et al. 2000, Black et al. 2002). In one of few studies that spanned multiple shears and storm strengths, Corbosiero and Molinari (2003), used lightning to deduce the effects of shear on the resulting asymmetric distribution of convection resulting from vertical wind shear.

A dominant pattern has emerged from these and other studies that describe the TC's response to forcing from vertical wind shear. This pattern consists of pronounced asymmetries, typically wavenumber one, in the pattern of vertical motion and the resultant precipitation field. In general, wind shear tends to produce anomalous upward motion downshear and anomalous downward motion upshear. The precipitation field appears to be strongly related to the direction and magnitude of the wind shear. This pattern has been noted in numerical modeling simulations with full physics that were then compared to observations (e. g., Rogers et al. 2003).

Most of the recent and current work on the effects of shear on the tropical cyclone focuses on modeled results and observations from individual storms. Structures vary between storms or even within a particular storm at different times during its life cycle. Notable differences in the shear-induced response of TCs have been reported among the numerical modeling community. It is difficult, therefore, to draw definitive conclusions based on individual snapshots from observations or output from a particular model. This work analyzes the vertical motion and precipitation structures from a variety of storms, undergoing differing magnitudes and directions of shear. The observations and analyses should provide a statistically robust data set for comparisons with analytical and numerical simulations of TCs interacting with environmental wind shear. In this short report, mean radius-height profiles of eyewall vertical motion and radar reflectivity are presented in relation to the large-scale shear.

2. OBSERVATIONAL DATA

The radar data set consists of Doppler velocities and reflectivities derived from vertically-pointing rays (vertical incidence or VI) recorded by the 3-cm tail radar system on the WP-3D aircraft. At intervals of ~750 m along the flight track, Doppler radial velocities and reflectivities are stored in 300 m vertical bins, from just above the sea surface to 15-km altitude. To estimate the vertical winds, the hydrometeor fallspeeds and the vertical motions of the aircraft are removed from the raw Doppler radial velocities. These procedures follow the methodology of Black et al. (1996), in which a subset of this data was used in a statistical study of vertical velocities.

To date, vertical incidence Doppler data have been processed for 224 radial legs, penetrations into or exits from the eye, that were obtained during 22 flights in 9 Atlantic and Eastern-Pacific hurricanes. The data set comprises a large range in hurricane intensity with wind speeds ranging from 40 m s^{-1} to 70 m s^{-1} and with minimum sea-level pressures varying from 970 to 892 mb

Initial calculations of vertical wind shear are from gridded analyses from the European Centre for Medium-Range Weather Forecasts (ECMWF) and provided by John Molinari from SUNY, Albany, NY. A more detailed description of the shear calculations may be found in Corbosiero and Molinari (2002).

**Corresponding author address* Michael L. Black, Hurricane Research Division, NOAA/AOML, 4301 Rickenbacker Causeway, Miami, FL 33149, Email: Michael.Black@noaa.gov

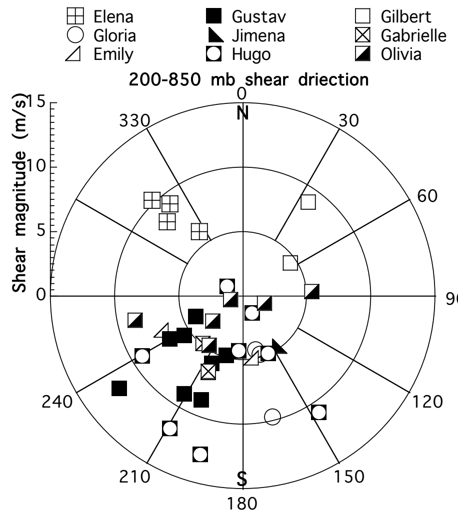

Figure 1: Magnitude and direction from which the environmental vertical wind shear is coming from for the 9 hurricanes listed at the top of the figure.

Figure 1 shows the distribution of the direction and magnitude of the vertical wind shear for the nearest times of the flights into individual hurricanes. Multiple values for an individual storm are because a combination of multiple flights cover more than one day and because shear values may be different for different times within a particular flight.

About two-thirds of the shear values in Fig. 1 are from the westerly direction, the prominent direction of environmental wind shear observed in the Atlantic basin. Of the westerly shear, nearly 80% is southwesterly. Shear from the east through the northeast is observed only rarely in this dataset. The magnitude of the shear is distributed more evenly than the direction with observed values <5 m s^{-1} occupying about 40% of the distribution. Large values of shear, >10 m /s, however, occur only in 5 of the 35 cases and in three hurricanes.

3. MEAN RADIUS-HEIGHT CROSS SECTIONS

For each flight, the distribution of radial legs were assigned to a quadrant, relative to the direction of the shear, downshear right and left, (DR, DL), and upshear right and left (UR, UL). Thus, if the shear was from the southwest and the radial leg was located in the eastern quadrant of the storm, the leg would be assigned to the DR quadrant. The total distribution of radial legs was fairly uniform, with 62, 60, 53, and 49 legs located in the DR, DL, UR, and UL quadrants, respectively.

In each shear-relative quadrant, simple radius-height means of reflectivity (dBZ) and vertical velocity (W) were constructed (Fig. 2) by averaging all the radial legs that were in each quadrant. The radius of a particular point was normalized by assigning the inner edge of the eyewall to a common radius for all of the profiles, This was done to account for differing sizes of the hurricanes' eye and considering that the sharpest gradients of wind speed and reflectivity are found along the inner eyewall edge.

The structure in the DL quadrant (Fig. 2a) has a pronounced radially-outward slope of the main updraft channel (30-50 km radius) and a prominent peak in radar reflectivity (>40 dBZ) near 7-km height

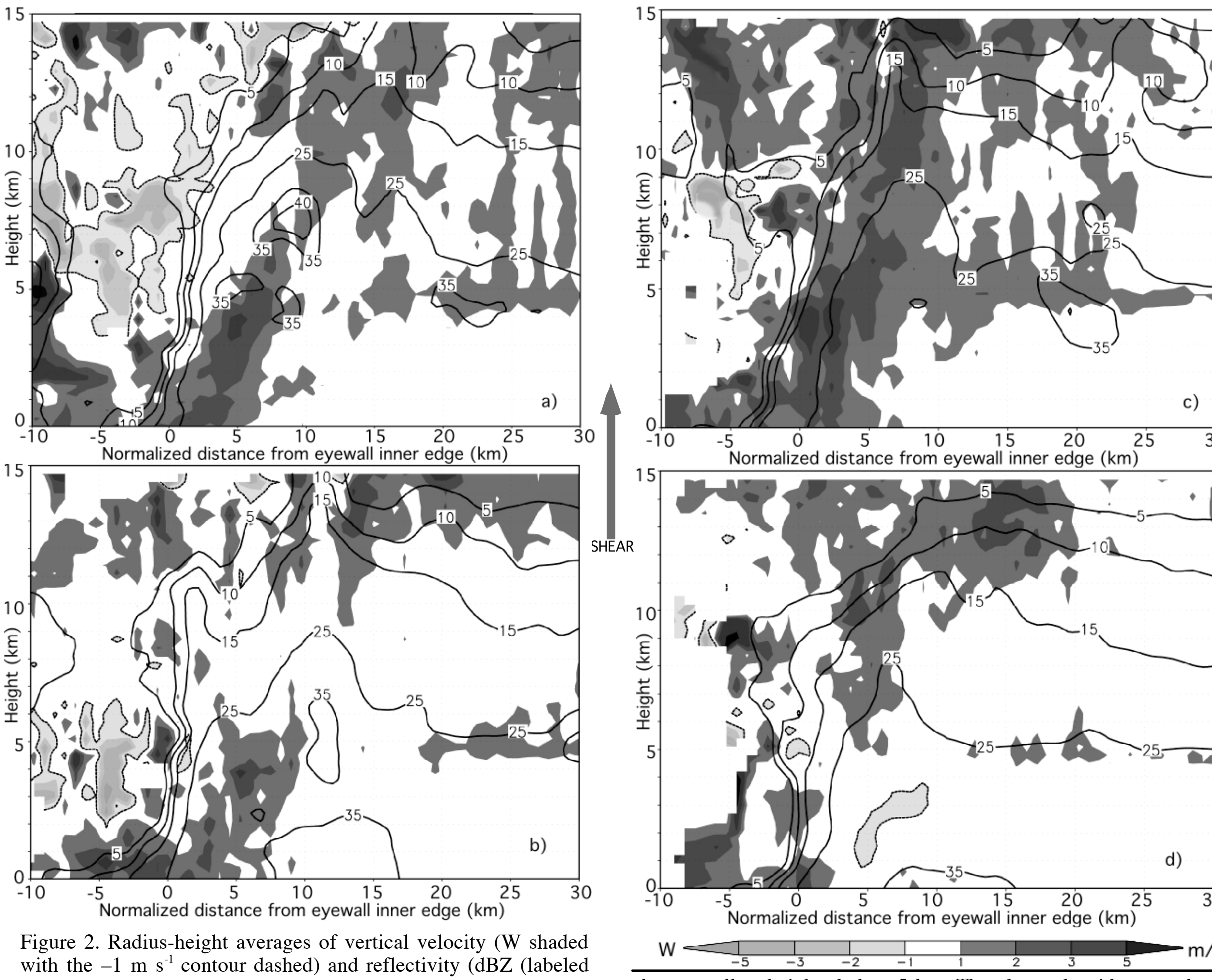

Figure 2. Radius-height averages of vertical velocity (W shaded with the –1 m s^{-1} contour dashed) and reflectivity (dBZ (labeled solid contours) for a) all radial legs in the a) DL, b) UL, c) DR, and d) UR quadrants relative to the shear. The radial legs were normalized in radius by placing the inner edge of eyewall for each leg at 30 km radius. The vertical velocity scale for all panels is at the bottom of d).

and 38-km radius. Somewhat surprisingly, the location of the strongest mean downward motion in the DL quadrant is along and inside of the inner edge of the eyewall and is strongest in the upper and mid- troposphere. Investigation of the individual profiles reveals that this strong downward motion occurs only in a small percentage of the radial legs in the stronger storms.

Overall, the strongest mean upward motion occurs in the DR quadrant (Fig. 2b) with a continuous updraft channel sloping outward throughout the depth of the troposphere. Secondary, substantial peaks of upward motion flank the main updraft channel in the upper troposphere. Unlike the DL sector, the DR quadrant has reflectivity that decreases more uniformly with height and has lower reflectivity values near the tropopause. In addition, the slope of the eyewall and main updraft channel is not as pronounced as the DL quadrant. In contrast, the mean reflectivity and vertical motion structures in the upshear quadrants (Figs. 2c, 2d) are substantially different than are observed downshear. In the UL quadrant (Fig. 2c), for example, the inner edge of the eyewall does not slope radially outward except at heights above 11 km. Here, the mean vertical motions are weaker with strong updrafts confined to the lower and upper troposphere and strong downdrafts located primarily inside of the eyewall at heights below 5 km. The elevated, mid-tropospheric reflectivity maximum is also observed in the UL quadrant but with values 10-15 dBZ lower than the DL quadrant.

The region of the eyewall that contains both the weakest mean vertical motion and reflectivity is in the UR quadrant (Fig, 2d). As in the UL quadrant, the slope of the eyewall in the mid and lower troposphere is nearly vertical. The reflectivity decreases most rapidly in this quadrant and echo tops (5 dBZ contour) are much lower than in all of the other quadrants. The strongest mean upward motion is broadly distributed in the upper troposphere and is confined near the inner edge of the eyewall at low levels. Mean downward motion in the UR sector is the weakest of all the quadrants, having a few small peaks at low altitudes below the weak eyewall reflectivity maximum and just inside of the eye at mid-to upper levels.

Together, these mean radius-height profiles show marked differences in the asymmetric structure of the eyewall as it relates to the environmental wind shear. The mean structures reported here are similar, but with notable differences as well, to those reported in numerical simulations and individual storm studies. It is the differences among the observations that are of the most interest and will be a focus of this ongoing research. Plans for future work include analyzing the frequency distributions of W and dBZ for each quadrant and to further stratify the data according to variations in the strength of the shear and the direction of the shear, relative to the storm motion.

4. REFERENCES

Available by request from the corresponding author